Ventilation of deep waters in the Adriatic and Ionian Seas following changes in thermohaline circulation of the Eastern Mediterranean

Beniamino B. Manca[1],*, **Valeria Ibello[2], Massimo Pacciaroni[1], Paolo Scarazzato[1], Alessandra Giorgetti[1]**

[1]Istituto Nazionale di Oceanografia e di Geofisica Sperimentale—OGS, Borgo Grotta Gigante 42/c, 34010 Sgonico (Trieste), Italy
[2]CNR, Istituto per le Scienze del Mare, Sezione di Trieste, Viale Romolo Gessi 2, 34123 Trieste, Italy

ABSTRACT: Hydrographic measurements obtained in March–April 2002 indicate a new ventilation of the deep layers in the Adriatic and Ionian Seas, following abrupt changes in the thermohaline circulation of the eastern Mediterranean observed since the beginning of the last decade. The water masses that reside in the Southern Adriatic basin were renewed by open ocean winter convection of water with potential density excess (σ_θ) > 29.18 kg m^{-3} at depths 600 to 800 m and by a vein of still denser (29.26 kg m^{-3}) and oxygen-rich (230 to 232 mmol m^{-3}) water flowing into the southern Adriatic depression (~1200 m), presumably from the north. When compared to 1999, a moderate increase in salinity (~0.05) and a much stronger dissolved oxygen increase (>29 mmol m^{-3}) were found in the bottom layer of the southern Adriatic Sea. The cold, fresh and highly oxygenated water of Adriatic origin, overflowing the Otranto Strait sill (~935 m) with a potential density of 29.24 kg m^{-3}, was dense enough to sink into the deep Ionian basin. Multiparameter analysis based on the fundamentals of the mixing processes was applied using temperature, salinity, oxygen and nutrient data to investigate the spatial distribution of water masses and to quantify the fractional contributions of distinctive source water types along specific sections running from the Adriatic to the Ionian Sea. The results clearly indicate that the dense water of Adriatic origin, which was recently in contact with the atmosphere, have again replenished the volume of the deep Ionian basin by more than 50%.

KEY WORDS: Ionian Sea · Adriatic Sea · Thermohaline circulation · Deep ventilation · Water mass composition

1. INTRODUCTION

Basin-wide hydrographic measurements obtained during the last 2 decades in the eastern Mediterranean have outlined important changes in the thermohaline circulation that deserve particular attention. The shift of dense water formation from the Adriatic to the Aegean Sea altered the deep internal conveyor belt as well as the physical and biogeochemical characteristics of the deep waters (Roether et al. 1996, Klein et al. 1999). It has been recognised that this major event, called the 'Eastern Mediterranean Transient' (EMT), was primarily related to the salinity increase in the

Aegean Sea (Malanotte-Rizzoli et al. 1999), which was initiated by the diversion of relatively fresh Atlantic water (AW) into the northern Ionian Sea owing to an anomalous surface forcing that occurred before 1987 (Pinardi et al. 1997). Observations conducted in 1987, 1991 and 1995 have indeed indicated a reduced transport of Atlantic water into the Levantine basin, where the salinity increased, and an altered circulation pattern of the Levantine Intermediate Water (LIW) from the formation site into the Ionian Sea (Klein et al. 1999, Malanotte-Rizzoli et al. 1999). These modifications in water characteristics, in addition to other factors mostly related to meteorological events (Lascaratos et al.

1999, Theocharis et al. 1999, Josey 2003), might have contributed to the formation of much denser waters in the Cretan Sea (south Aegean) relative to the waters traditionally formed in the Adriatic Sea. Moreover, the nutricline was elevated closer to the photic zone, thus making more nutrients available for consumption or transport owing to upper ocean dynamics. Most importantly for the marine ecosystem, the transient event (EMT) increased the oxygen concentration in the bottom layer of the central region with respect to the 1987 situation (Klein et al. 1999).

Since 1997, the EMT has undergone an important evolution. Evidence exists for the disappearance or absence of new replenishment of the bottom layer of the eastern Mediterranean (Manca & Scarazzato 2001, Theocharis et al. 2002) while the Aegean contribution was of lesser density, flowing at mid-depths (~2000 m). Moreover, the already-discharged bottom waters extended prevalently eastward into the Levantine basin, where an increase of oxygen was noticed in 1999 (Kress et al. 2003).

However, within the period 1995 to 1999, the total amount of oxygen decreased by about 5 µmol kg^{-1} with respect to the transitional (500 to 1000 m) and bottom (>2200 m) layers. This phenomenon, if converted into utilization rate, implies an oxygen consumption increase of about 1.3 µmol (kg yr)$^{-1}$, probably related to the large intrusion of dissolved organic carbon with a high fraction of labile material (Klein et al. 2003, Seritti et al. 2003).

In the Ionian Sea, the observations performed in 1999, if compared to those in 1995, revealed strong changes in dynamics, which further influenced the properties of the water masses and the structure of the water column (Manca et al. 2003). In the upper layer, the meandering current systems restored the transport of relatively fresh Atlantic water mainly into the Levantine basin rather than into the northern Ionian. The intermediate layer, traditionally occupied by the LIW, appeared to be mostly influenced by a much more saline and oxygenated water type supplied by the Cretan Sea, the Cretan Intermediate Water (CIW). This latter water mass, spreading prevalently northward at the 29.05 kg m^{-3} isopycnal, flowed into the Adriatic Sea where the salt content increase was consistent with changes in the Ionian dynamics. In the deep layer, salinities increased in the northern and western Ionian and decreased around the Cretan Arc Straits owing to the spreading of the dense Aegean-derived waters far away from the central region.

In this study, we present results from investigations conducted in the Ionian and Adriatic Seas in 2002. These measurements were interpreted from the perspective of interannual variations in winter climatic and oceanographic conditions in the eastern Medi-

terranean, and provided experimental evidence for related changes in the large scale circulation patterns and water mass structures upon the EMT. In particular, cold, fresh and highly oxygenated waters of Adriatic origin, overflowing the Otranto Strait, were dense enough (~29.24 kg m^{-3}) to sink into the Ionian abyssal layer. This study also discloses the physical and chemical properties of distinctive source water types, which are utilised in the multiparameter analysis to calculate the mass fractions along specific sections in the Ionian Sea. These quantities might be related to biochemical patterns in future studies conducted in order to draw firm conclusions on whether the EMT has triggered an increase in biological production, nutrient consumptions and accelerated oxidative processes of organic matter.

This study is structured as follows. Section 2 briefly reviews the hydrographic data used, their distribution and methods of analysis. Section 3 discusses the hydrographic patterns and water mass dynamics by means of vertical sections, horizontal and isopycnal analyses. Section 4 presents the generic background on optimum multiparameter analysis, the quantitative mass fractions and mixing of distinctive source water-types identified in the Ionian and Adriatic Seas. Finally, long-term changes in the water column structure are studied by comparison of hydrographic data from 2 synoptic surveys carried out in 1999 and 2002. Section 5 provides a summary and some concluding remarks.

2. DATA SETS AND METHODS

Hydrographic observations conducted aboard RV 'Urania' during the SINAPSI-4 cruise from 27 March to 10 April 2002 provided a medium-resolution survey covering 29 positions in the northern Ionian and southern Adriatic Seas. In order to present basic hydrographic features at the intermediate and deep layers over a broader region, CTD stations in the southern Ionian from the RV 'Meteor' cruise of November 2001 are included. The comparison of CTD casts during the 2 surveys at the same positions exhibits no large discrepancies in the intermediate and deep layers, making possible the use of the combined datasets. The topography of the investigated area and locations of hydrological stations are displayed in Fig. 1. The station spacing for both cruises was aimed at investigating basin-scale changes in water mass characteristics and biochemical features, mostly associated with the evolution of the great Aegean anomaly.

A Seabird SBE 911-plus CTD rosette system, equipped with 24 conventional 10 l Niskin bottles, was lowered at each station of both cruises and covered the full water column. Temperature and salinity measure-
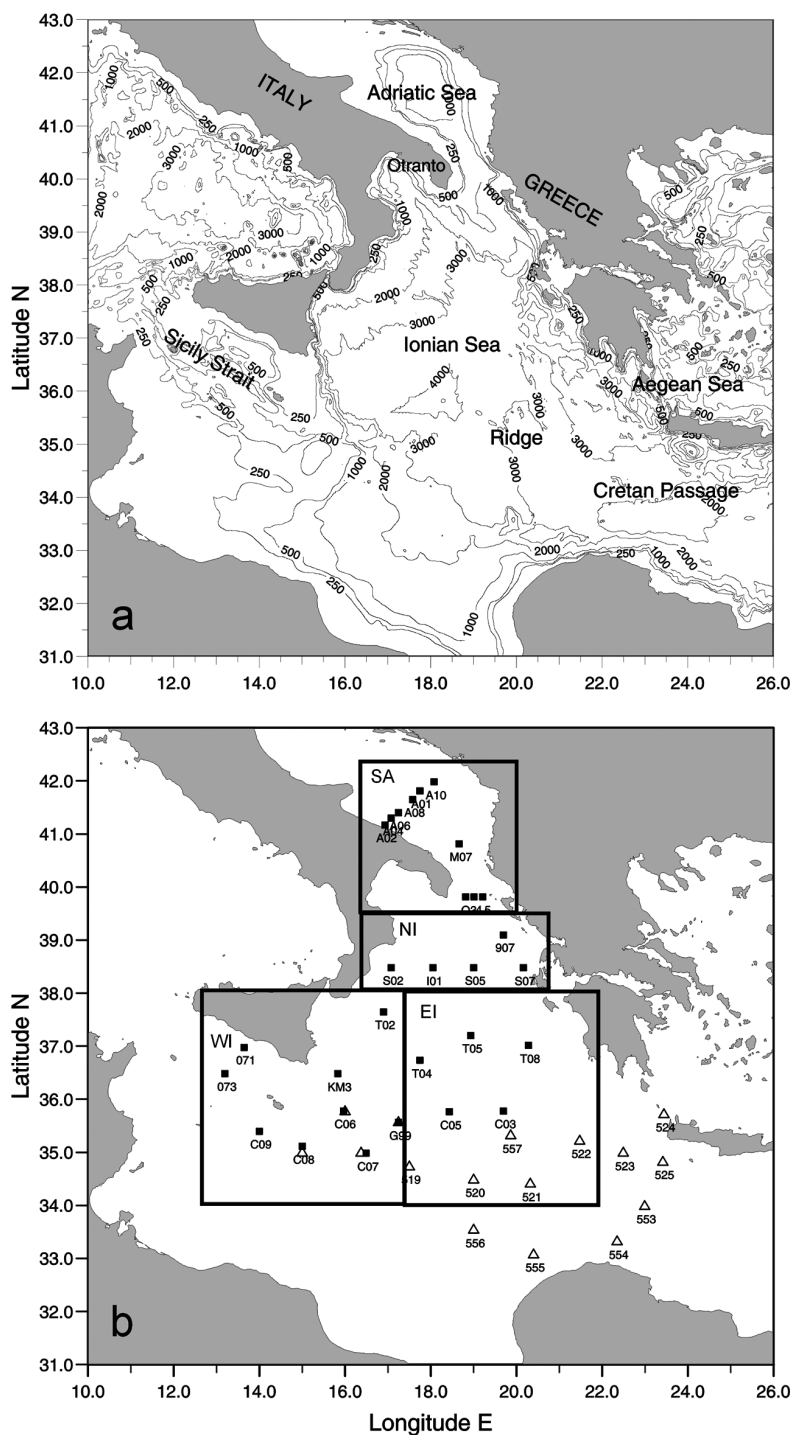
Fig. 1. (a) Bottom topography of the Ionian and southern Adriatic Seas; (b) location of CTD stations (boxed) occupied during SINAPSI-4 (RV 'Urania'), 27 Mar–10 Apr 2002 (■) and M51/2 (RV 'Meteor'), 18 Oct–11 Nov 2001 (△). Principal topographic features indicated in m

perature and salinity data were obtained by duplicate sensors concurrently controlled during the cruise and calibrated on land before and after the cruise. The discrepancies were within ±0.002 units. In the following, the temperature is reported as potential temperature (θ), salinity (S) is expressed on the practical salinity scale 1978, and the derived potential density excess (σ_θ) refers to the sea surface. Horizontal maps were constructed at the indicated depth by extracting bin-averaged values over 1 dbar intervals, and interpolating them onto a regular grid using objective analysis. An isotropic correlation function was used (Carter & Robinson 1987); the zero crossing and the spatial correlation length scale were 180 and 100 km, respectively. Areas where the expected error variance exceeded 40% were not plotted.

Water samples for oxygen measurements were collected and analysed on board using a Metrohm burette and the Winkler procedure (Carpenter 1965). The final point was automatically determined by means of a redox electrode. The coefficient of variation $(CV\,[\%] = 100 \times [SD \times mean^{-1}])$ on replicates was better than 0.4%. In addition, the continuous dissolved oxygen measurements obtained along the water column by means of a polarographic sensor fitted to the CTD case were corrected against the discrete Winkler determinations at each station. Discrepancies after correction between the 2 data sets were within 0.3%.

Water samples for dissolved inorganic nutrient determinations were collected in 25 ml polyethylene vials, immediately frozen at –20°C and subsequently analysed in the laboratory. Nitrite, nitrate and silicate were measured with a hybrid auto-analyser equipped with a Chemlab continuous flow colorimeter according to the method of Grasshoff et al. (1983) with slight modifications. Phosphate was measured with a hybrid auto-analyser equipped with a Technicon continuous flow colorimeter. The CV was better than 2%.

This study discusses results obtained by temperature, salinity and oxygen measurements. Nutrient data from the RV 'Urania' cruise are used to quantify fractions of distinctive source water types in the Ionian and Adriatic Seas by applying the optimum multiparameter (OMP) analysis in its basic formulation (Tomczak 1981).

ments were supplemented with those of dissolved oxygen, transmittance and fluorescence. During the up-cast, water samples were collected for oxygen, nutrients, biological and tracer determinations. Tem-

3. RESULTS

CTD data were interpolated along 2 zonal sections to illustrate the vertical distribution of oceanographic properties in the centre of the Ionian and Adriatic Seas (Figs. 2 & 3) and in 2 meridional sections connecting the 2 basins at nominal latitudes of 20° E (Fig. 4) and 17° E (Fig. 5), chosen according to the spreading of the principal water masses.

3.1. Vertical distribution of water masses in upper, intermediate and deep layers

In the Ionian section (Fig. 2), the striking features in the upper layer (<200 m) are AW to the west and a more saline core water to the east. The AW spreads from the Sicily Straits to the east whereas the more saline core water intrudes into the Ionian from the eastern side and flows prevalently northwards, according to the general cyclonic character of the interior dynamics. This latter water mass mixes with the AW and becomes the Ionian Surface Water (ISW).

At the intermediate depth (200 to 800 m), the well-distinguished salinity maximum (S > 38.80) indicates advective propagation of the highly saline LIW/CIW. The distinction between LIW and CIW cannot be easily identified in the salinity distribution, but becomes clearer in the composite property-property plots of the biochemical parameters shown in Section 4. However, the CIW, which is characterised by the more saline patches, lies in the upper portion of this layer and results in more ventilated water than the LIW.

In the deep layer (>1000 m), the decrease in salinity and increase in oxygen (Fig. 2, lower panels) indicates the presence of relatively fresh and recently ventilated water of Adriatic origin. This water exiting through the Otranto Strait extends much further westwards due to Coriolis forcing and, upon sinking, accumulates in the Ionian abyssal layer where it mixes with ambient water to become the Eastern Mediterranean Deep Water (EMDW). However, the sloping isolines from west to east indicate the contemporary presence of waters of Adriatic and Aegean origin. In fact, the Adriatic water is laterally bounded by a water mass that is relatively warmer (not shown), saltier but less ventilated centred at ~2000 m, i.e. the Cretan Deep Water (CDW), discharged at shallower depths due to evolution of the EMT (Manca & Scarazzato 2001, Theocharis et al. 2002).

Finally, in the layer below the LIW and above the more ventilated deep water, low oxygen values indicate the Transitional Mediterranean Water (TMW) that can be traced in the whole eastern Mediterranean at shallower depths (between 800 and 1500 m) as a consequence of the deep intrusion of denser Aegean-derived waters (Klein et al. 1999, Theocharis et al.
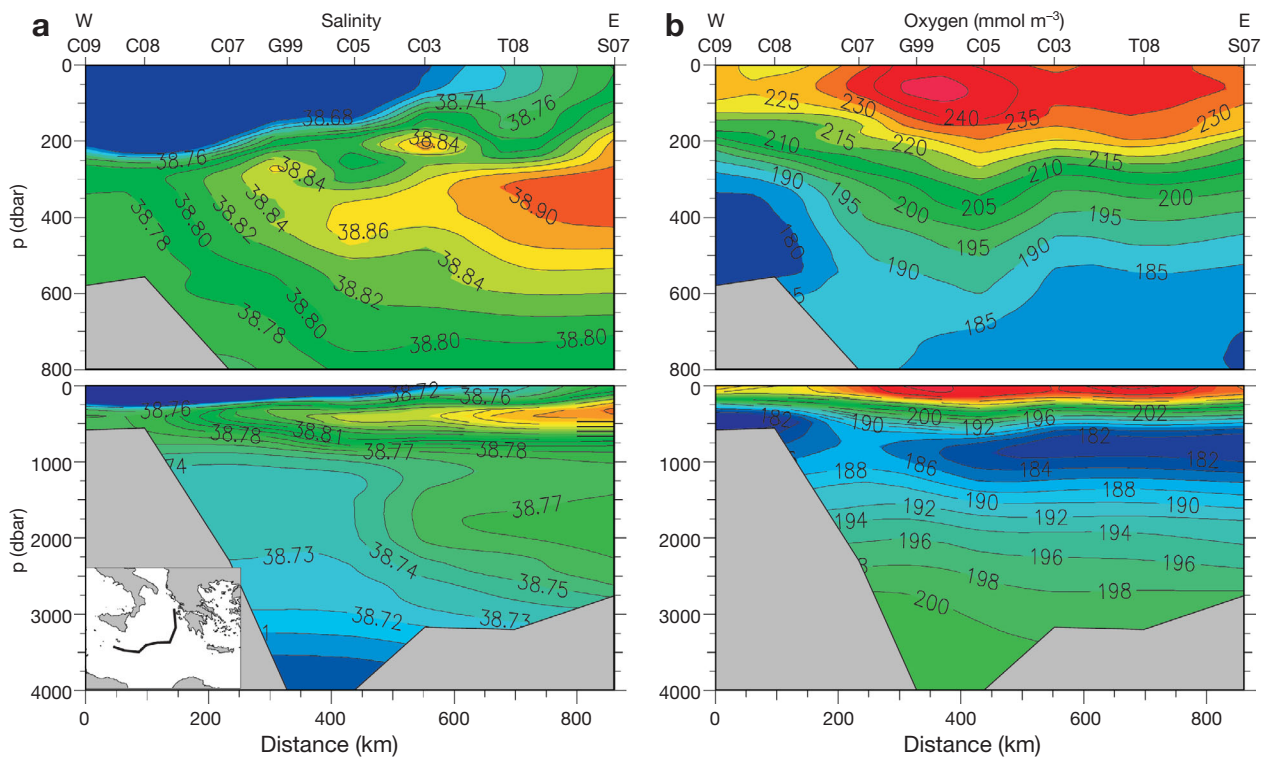

Fig. 2. Vertical distributions of (a) salinity and (b) oxygen (mmol m^{-3}) along the section at nominal latitude 36° N (inserted map). Upper panels highlight the first 800 m. Positions of CTD stations indicated at the top of the x-axis

2002, Kress et al. 2003). The salinities in this depth interval are systematically lower than those in the intermediate layer, while the oxygen minima indicate that this layer is scarcely renewed. Therefore, the diapycnal mixing between the overlying highly saline and the underlying less saline water masses could be the unique mechanism able to modify the TMW. In contrast, the deep Ionian basin becomes rather well-ventilated by the advective propagation of much denser waters of either Adriatic and/or Aegean origin.

The southern Adriatic deserves attention, as it is the region where the production of the Adriatic Deep Water (ADW) takes place by open-ocean deep convection. In 2002, the most prominent features observed along the transect crossing the southern Adriatic depression were (Fig. 3): (1) the signal associated with the highly saline CIW/LIW that intrudes into the Adriatic Sea in the upper layer (Fig. 3b); (2) the front on the western slope generated by the arrival of the cold, less saline and oxygen-rich (Fig. 3a–c) North Adriatic Dense Water (NADW); (3) the ventilation of the bottom layer, never observed during the last 2 decades (Fig. 3c); and (4) the presence of a nepheloid layer, which extends from the western slope to the bottom layer (Fig. 3d). Thus, the vertical distribution of the oceanographic properties exhibits features different

from the usual these latter were mainly characterised by a tongue of highly saline waters in the intermediate layer (Artegiani et al. 1997) and by low oxygen and high nutrient concentrations below 1000 m owing to the longer residence time of the water mass in the deep trench (Manca et al. 2004).

In the upper layer, the stratified conditions, exemplified by the temperature field (Fig. 3a), were re-established during the early spring, overlaying the recently ventilated waters in the deeper layer. The deep ventilation, as seen from the high oxygen content in the centre of the basin (Fig. 3c), might have originated from the surface via deep convection and from the edges of the density-driven bottom current that transports dense waters from the northern region. In 2002, while the former process reached depths 500 to 800 m at Stn A01, the much denser water flowing from the north may have survived the deepening in the middle Adriatic depression (as observed by Marini et al. 2006, this issue), and upon reaching the shelf break sank into the southern Adriatic depression. Low oxygen patches at the border of the convection region are associated with older deep-waters re-circulating in the southern gyre before their complete mixing. The optical characteristics of the bottom waters (Fig. 3d) further support this interpretation. The nepheloid layer could be gen-
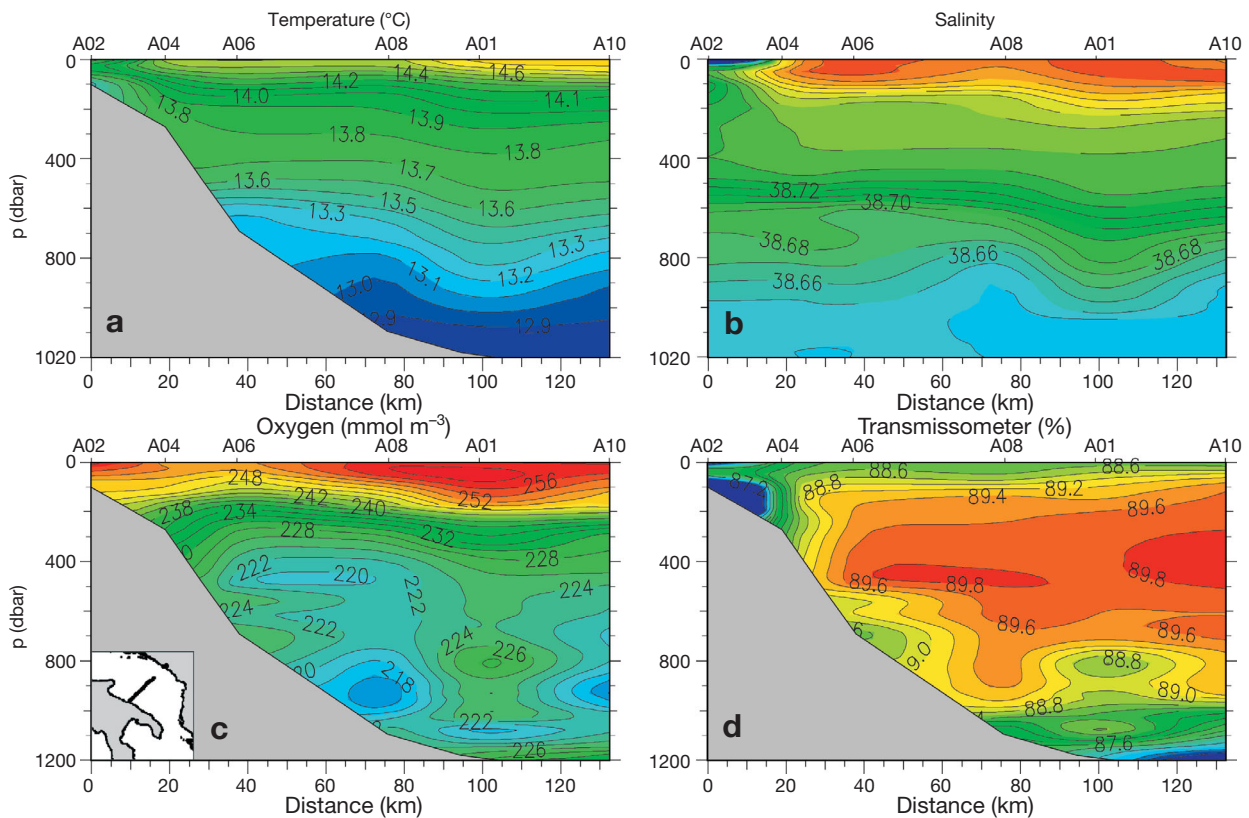

Fig. 3. Vertical distributions of (a) temperature (°C), (b) salinity, (c) oxygen (mmol m^{-3}) and (d) light transmission (%) along the east-west section crossing the southern Adriatic depression (inserted map). Positions of CTD stations indicated at the top of the x-axis

erated by the re-suspension of fine sediments due to the bottom current and/or by waters of riverine input flowing from the north; in contrast, clearer waters are present in the convection region.

Figs. 4 & 5 depict the longitudinal sections that link the southern Adriatic and Ionian Seas along the Greek and Italian coasts, respectively. These sections are constructed using the same stations in the Adriatic, while the southern stations are the same as those at the eastern and western ends of the zonal section illustrated in Fig. 2. The surface and intermediate layers are occupied by the highly saline ISW and LIW/CIW, respectively. These water masses penetrate extensively into the Adriatic Sea, and the core of the salinity maximum becomes much more elevated because of the cyclonic circulation in this region. In the deep layer, a pronounced salinity front is established in the Otranto Strait between the relatively fresh and highly oxygenated ADW to the north and the salty and less oxygenated Ionian waters to the south. The oxygen minimum layer indicates the TMW sandwiched between the LIW/CIW and the more recently ventilated deep water of Aegean or Adriatic origin. The gradual advance of the more saline CDW toward the Adriatic is obstructed by the topography in the eastern section (Fig. 4), where the Aegean contribution appears prominent at 2000 m. On the other hand, the deep waters characterised by salinity minima and high oxy-

gen content clearly extend from the Adriatic into the Ionian Sea in the western section (Fig. 5).

From the analyses of the 3 sections constructed in the Ionian Sea, one notes that the Adriatic signature, characterised by low salinities and high oxygen contents, may be recognised over the sill depth at the Otranto Strait (~935 m) and is still present, even if slightly modified, up to Stn S02 in the Ionian Sea. Although the Adriatic influence is minor downstream at Stn T02, deep salinity minima (S ~38.69) and high oxygen values (O_2 ~200 mmol m^{-3}) are again seen at the bottom of the southernmost stations in the Ionian abyssal plain (Figs. 2 & 5). Evidently, the Adriatic waters are transported southward against the western continental slope in a boundary current 'coastally trapped' at depth levels between 1000 and 2000 dbar, as was observed in 1999 from a more appropriate station distribution (Manca et al. 2003). In synthesis, the spatial structure of the hydrographic field shows a gradual intrusion in the deep layer of Adriatic dense waters that mix with the ambient deep water of Aegean origin. However, the former still dominates in the Ionian abyssal layer, as indicated by the thick homogenous layer marked by low salinity, low potential temperature (not shown) and high-oxygen concentrations (Figs. 2, 4 & 5).

A coherent account of the change in deep-water hydrography, as observed in the Ionian basin in 2002, can be inferred from the oxygen concentrations with reference to the values of 207 and 193 µmol kg^{-1}
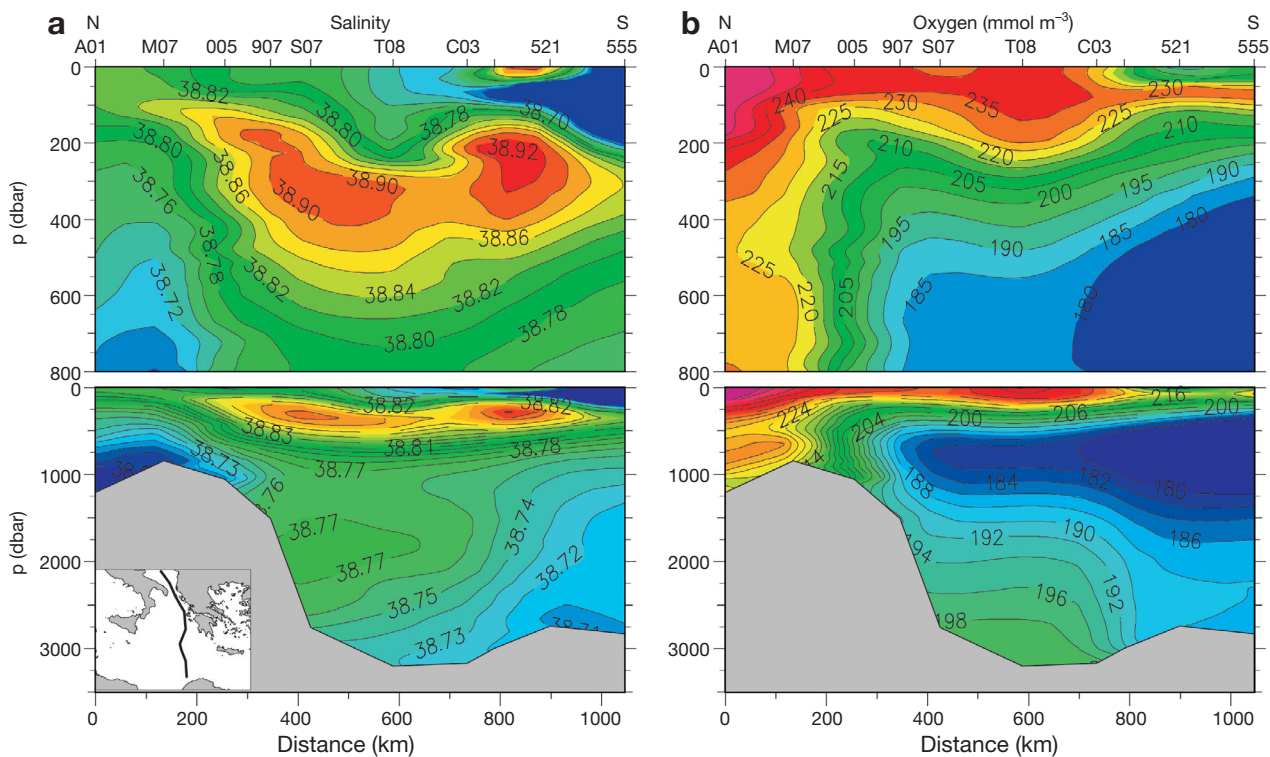

Fig. 4. Vertical distributions of (a) salinity and (b) oxygen (mmol m^{-3}) for the north-south section at 19–20° E in the eastern Ionian Sea (inserted map). Upper panels highlight the first 800 m. Positions of CTD stations indicated at the top of the x-axis

observed in 1987 by Schlitzer et al. (1991) in the western and central Ionian, respectively. On the basis of the oxygen consumption rate of R = 0.53 µmol $(kg^{-1} yr^{-1})$ calculated by Roether & Well (2001), these values if converted in volumetric concentrations should result in about 200 and 185 mmol m^{-3} in 2002. The higher values (i.e. 209 and 200 µM) should not be possible without a new substantial replenishment by the Adriatic Sea.

3.2. Horizontal distributions of thermohaline properties in upper, intermediate and deep layers

The horizontal distributions of temperature and salinity fields in the surface layer (Fig. 6a,b) demonstrate the lateral extent of the AW and ISW in the studied region. In order to eliminate any possible 'skin effect' in this representation, data were averaged over a depth interval of 10 m. It is worthwhile remarking that, in winter, the core of the AW is at the surface and occupies most of the upper layer (Hopkins 1978). The hydrographic patterns indicate a flow of high temperature and low salinity waters that move from the Sicily Strait into the southern Ionian Sea. In contrast, warm and saline waters enter the Ionian from the east and flow northwards along the Greek coast. A sharp temperature and salinity front at 36° N divides the ISW in the north from the AW to the south, where it flows prevalently eastwards by an anticy-

clonic motion (Fig. 6d). The ISW is laterally bounded on its western side by a water mass characterised by low temperature and high salinity. This is probably caused by the dynamics, which manifest a broad cyclonic character in the Ionian interior (Fig. 6d), so that cold and salty waters are elevated from the intermediate layer close to the surface (Figs. 5a & 6a,b). The density gradients (Fig. 6c) manifest the same west-east orientation of the isolines in the south indicating the eastward flow of the AW, whereas they assume a north-south orientation in the north due to the northward flow of the ISW that extends into the Adriatic Sea.

The distributions of temperature, salinity and oxygen at the 29.05 kg m^{-3} isopycnal (Fig. 7a–c) are used to illustrate the hydrographic patterns in the intermediate layer, whereas the topography of such an isopycnal (Fig. 7d) is mostly indicative of the dynamics. The signal associated with the LIW is recognizable by low temperature, salinity and oxygen values at the eastern entrance of the Ionian Sea. The LIW flows prevalently through the Cretan Passage towards the Sicily Straits. Pure CIW, characterised by patches of higher temperature and salinity values, emanates from the western Cretan Straits and flows prevalently northwards along the Greek coasts, establishing a meridional front with a less saline and more oxygenated intermediate water to the west. However, mixtures of LIW and CIW take place at lower densities and spread into the Ionian interior.
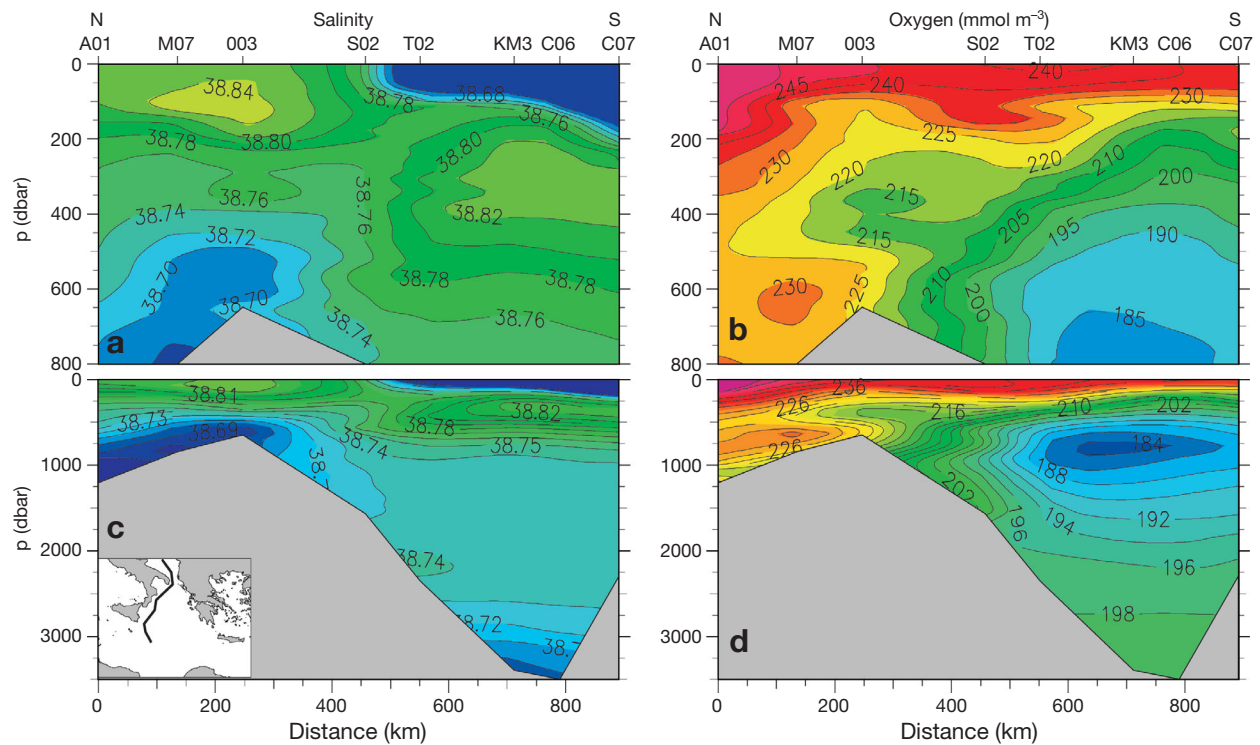

Fig. 5. Vertical distributions of (a & c) salinity and (b & d) oxygen (mmol m^{-3}) for the north-south section at 16–18° E in the western Ionian Sea (inserted map). a & b highlight the first 800 m. Positions of CTD stations are indicated at the top of the x-axis
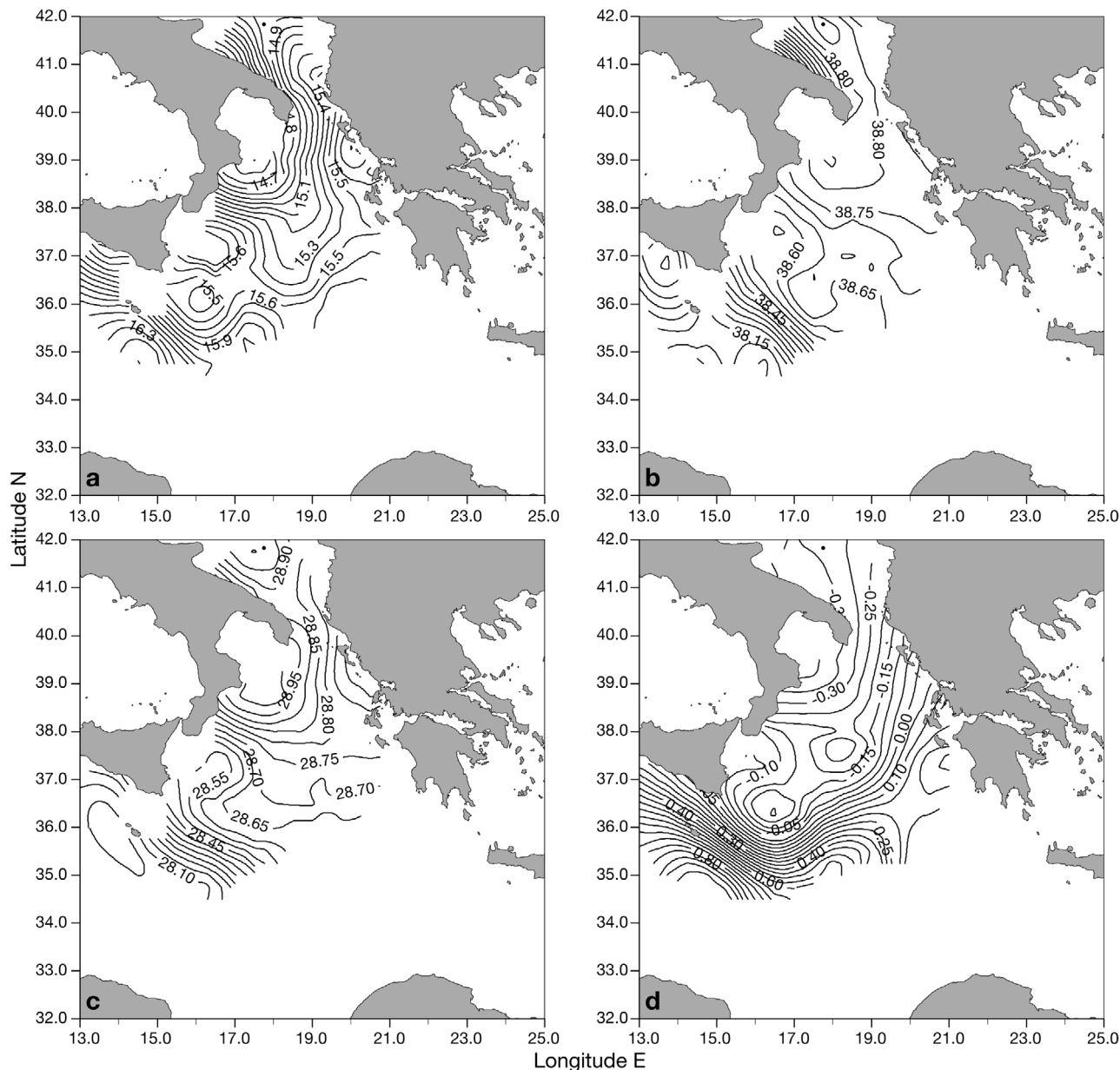
Fig. 6. Horizontal distributions of (a) temperature (°C), (b) salinity, (c) density (kg m^{-3}) at the surface and (d) geopotential anomaly (m^2 s^{-2}) relative to 250 dbar in Mar–Apr 2002, SINAPSI-4 cruise. For sampling station positions see Fig. 1b

The depth of the 29.05 kg m^{-3} isopycnal is shallower in the north and deeper in the south (Fig. 7d). This feature is well correlated with the large-scale cyclonic circulation at the surface (Fig. 6d), which extends to the intermediate layer. Moreover, sub-basin-scale cyclonic and anticyclonic eddies superimpose at this depth, such as those centred at about 34° N, 23° E and 35° N, 19° E, respectively. The latter exhibits a strong barotropic character that involves the density range 28.80 to 29.15 kg m^{-3} (not shown) entraining warm, saline and more oxygenated CIW to greater depths (>400 m).

4. QUANTITATIVE WATER MASS ANALYSIS

4.1. Issues addressing water mass fractions, transformation and mixing in the Ionian Sea

The relative contributions of various water masses to a water sample have been estimated by using the OMP analysis described by Tomczak & Large (1989). According to its basic assumption, each seawater parcel (sample) can be considered as a mixture of selected Source Water Types (SWTs), whose fractions are calculated by solving the overdetermined linear system of
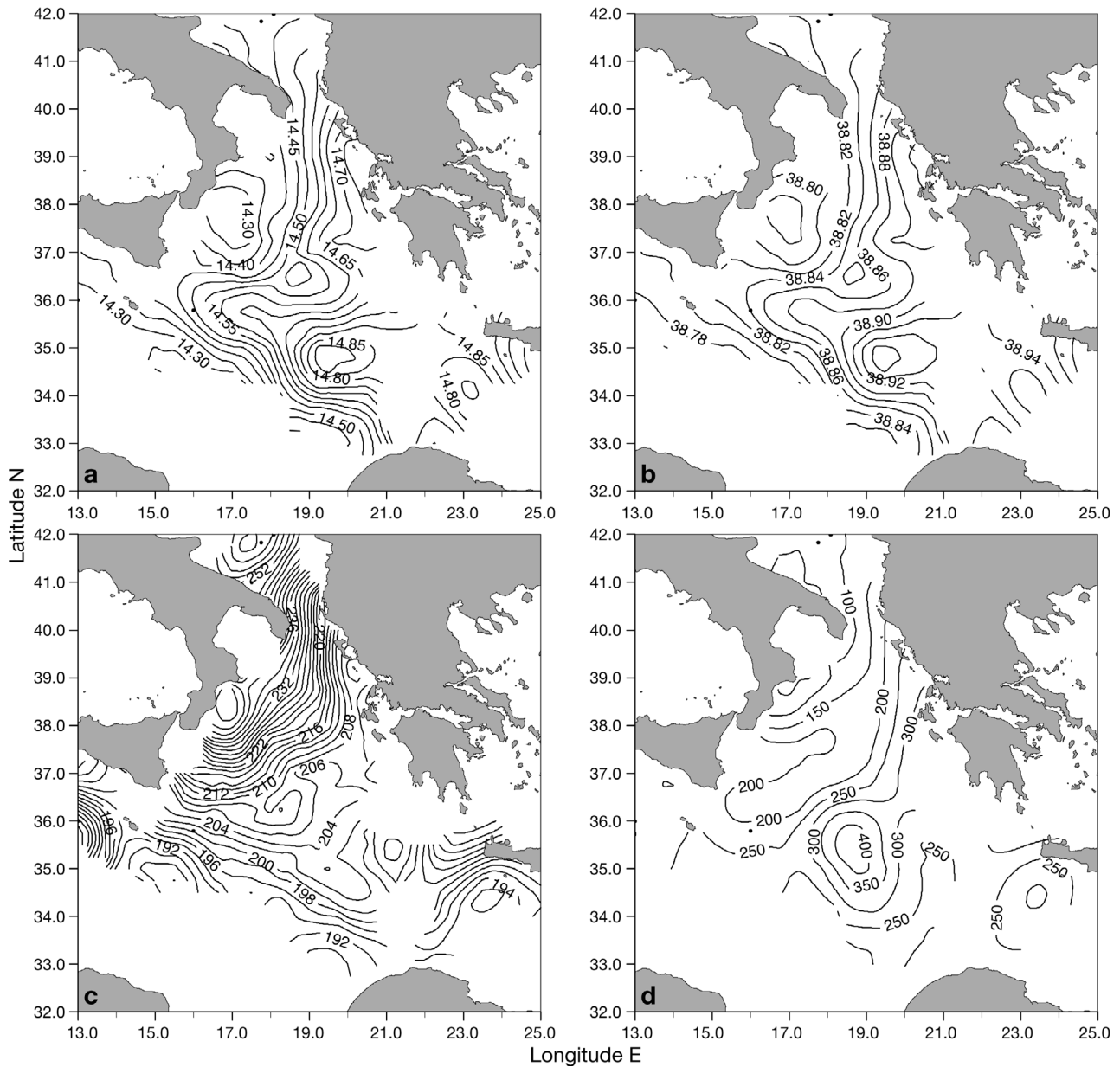
Fig. 7. Horizontal maps of (a) temperature (°C), (b) salinity, (c) dissolved oxygen (mmol m^{-3}) and (d) depth (m) at 29.05 kg m^{-3} isopycnal. Maps obtained using CTD data collected Mar–Apr 2002 (RV 'Urania') combined with data collected Nov 2001 (RV 'Meteor'). The isopycnal is the typical horizon for the spreading of the LIW/CIW core. For sampling station positions see Fig. 1b

mixing equations. Thus, each water sample can be represented in the linear system by one or more SWTs under the assumption that the local variability in properties derives from mixing and exchange processes, exclusively.

Since our discussion involves more than 3 water types, in order to overcome the major limitation imposed by using solely temperature and salinity (in which case only 3 water types can be employed), we have used the nutrient parameters considered as independent and conservative tracers (to some extent).

Since our analysis is conducted over a limited ocean region, the rather restricted temporal scales of the involved advective-diffusive processes prevail over biochemically induced concentration changes, making possible the use of nutrients as conservative tracers (Leffanue & Tomczak 2004). Moreover, concerning the distribution of nutrients in Mediterranean waters, many authors have emphasised the peculiar biochemistry of this sea, reporting, for example, enhanced deep respiration and non-Redfieldian behaviour of nutrient ratios (Bethoux 1989, Kress & Herut 2001, Roether &

Well 2001, Kress et al. 2003, Ribera d'Alcalà et al. 2003). The nutrient ratios in Mediterranean Sea display anomalous values that are always higher than those for the oceans. This is mainly due to (1) the relevant internal dynamics of the sea and (2) the presence of many source water masses of different ages (Kress et al. 2003). In this case, nutrient concentrations become independent variables and can be used as tracers to re-construct internal dynamics of the basin (Bethoux et al. 1992).

The source water types considered in the Ionian and Adriatic Seas are: the Atlantic Water (AW), the Ionian Surface Water (ISW), the Levantine Intermediate Water (LIW), the Cretan Intermediate Water (CIW), the Transitional Mediterranean Water (TMW), the Adriatic Deep Water (ADW), the Eastern Mediterranean Deep Water (EMDW) and the Cretan Deep Water (CDW). Given the high number of SWTs (eight), we use oxygen and nutrients (nitrate, phosphate and silicate) in addition to temperature, salinity and potential vorticity, for the parameters; the latter has been included under the assumption that the flow field is in quasi-geostrophic equilibrium.

The resulting linear system of equations is:

$$
\begin{aligned}
x_1\theta_1 &+ x_2\theta_2 + x_3\theta_3 + x_4\theta_4 + x_5\theta_5 + x_6\theta_6 + x_7\theta_7 + x_8\theta_8 = \theta_{obs} &+ R_\theta \\
x_1S_1 &+ x_2S_2 + x_3S_3 + x_4S_4 + x_5S_5 + x_6S_6 + x_7S_7 + x_8S_8 = S_{obs} &+ R_S \\
x_1O_1 &+ x_2O_2 + x_3O_3 + x_4O_4 + x_5O_5 + x_6O_6 + x_7O_7 + x_8O_8 = O_{obs} &+ R_O \\
x_1P_1 &+ x_2P_2 + x_3P_3 + x_4P_4 + x_5P_5 + x_6P_6 + x_7P_7 + x_8P_8 = P_{obs} &+ R_P \\
x_1N_1 &+ x_2N_2 + x_3N_3 + x_4N_4 + x_5N_5 + x_6N_6 + x_7N_7 + x_8N_8 = N_{obs} &+ R_N \\
x_1Si_1 &+ x_2Si_2 + x_3Si_3 + x_4Si_4 + x_5Si_5 + x_6Si_6 + x_7Si_7 + x_8Si_8 = Si_{obs} &+ R_{Si} \\
x_1Pv_1 &+ x_2Pv_2 + x_3Pv_3 + x_4Pv_4 + x_5Pv_5 + x_6Pv_6 + x_7Pv_7 + x_8Pv_8 = Pv_{obs} &+ R_{Pv} \\
x_1 &+ x_2 + x_3 + x_4 + x_5 + x_6 + x_7 + x_8 = 1 &+ R_{Mc}
\end{aligned}
$$

Each column corresponds to 1 SWT defined by θ_i (potential temperature), S_i (salinity), O_i (oxygen), P_i (phosphate), N_i (nitrate), Si_i (silicate), Pv_i (potential vorticity) and Mc (mass conservation). The last equation accounts for the condition of Mc. The x_i vector stands for the water mass fractions ($0 \le x_i \le 1$) of each SWT that best describe the composition of the water sample as derived from the observations (θ_{obs}, S_{obs}, O_{obs}, P_{obs}, N_{obs}, Si_{obs}, Pv_{obs}). The Mc equation and non-negativity of the solutions are introduced as physical constraints. The linear system is solved by minimising the residuals (R) in a weighted least-squares sense (Mackas et al. 1987), after normalizing the matrix of SWTs and weighting the contribution of each parameter because of different accuracies.

The SWTs were defined from the hydrographic data at the stations closest to the respective source regions. The physical characteristics were defined from the θ-S diagrams (Fig. 8) constructed using full depth CTD data and grouping together the stations located in 4 main regions (Fig. 1b): the southern Adriatic including the Otranto Strait, the northern Ionian, the western and the eastern Ionian. The property-property plots of potential temperature versus dissolved oxygen, nitrate, phosphate and silicate are constructed from bottle data (Fig. 9).

In the western Ionian (Fig. 8c), the salinity and temperature values of the AW range from 37.6 to 38.6 and from 15 to 17°C, respectively. It occupies the layer 0 to 150 m at stations C09, C08, C07 and may be still recognized at Stn C06, while a hint of AW appears at stations T02, KM3 and G99 (see Fig. 1b for station positions). The AW, as it moves eastward, mixes with the more saline ISW, which is well identified in the eastern and northern Ionian (Fig. 8b,d) by salinities greater than 38.70. As stated above, the ISW occupies a much broader region and has density values lower than 28.8 kg m⁻³. The 28.8 isopycnal is situated at 150 m at latitude 36° N; it deepens to 250 to 300 m at Stn CO5 (not shown) due to the presence of an anticyclonic eddy, and surfaces in the northern Ionian.

Moving into the intermediate layer and below the pycnocline (28.8 to 29.0 kg m⁻³), 2 deviations towards high salinity values identify the CIW and LIW. The CIW has salinity always greater than 38.90 (Fig. 8b,c), whereas the temperature ranges from 14.5 to 15.5°C and density from 29.0 to 29.1 kg m⁻³. The LIW has salinity and temperature values lower than the CIW: its core is characterised by temperatures from 14.0 to 14.5°C, salinities of about 38.85 and a density in the range of 29.05 to 29.15 kg m⁻³. Therefore, the LIW occupies a deeper layer situated at 250 to 600 m.

Underneath, the TMW has no specific signature in the θ-S diagrams. It is biochemically defined from extremes in the property-property plots in Fig. 9. However, its core—defined by the oxygen minimum layer (OML)—lies at about 750 m and has an average temperature and salinity of 13.75°C and 38.75, respectively.

In the deep layer ($\sigma_\theta > 29.17$ kg m⁻³), the steady decrease of potential temperature and salinity provides clear evidence for the prevailing advection path of less saline and colder ADW. The ADW at the Otranto Strait has properties of $\theta = 12.92$°C, S = 38.64, $\sigma_\theta =$ 29.24 kg m⁻³ and O₂ ~ 230 mmol m⁻³ (Figs. 8a & 9a). During the overflow through the strait into the Ionian abyssal layer, the ADW mixes with the ambient water. Hereby, the new and more homogeneous water type, the EMDW, shows near-bottom properties of $\theta =$ 13.28°C, S = 38.69 and $\sigma_\theta =$ 29.20 kg m⁻³. These properties are quite similar to those observed in 1987 (Schlitzer et al. 1991), only differing in a higher oxygen concentration (O₂ = 200 mmol m⁻³). At Stn T08 in the eastern Ionian, small modifications from the EMDW toward higher temperature and salinity values ($\theta =$ 13.60°C, S = 38.78, $\sigma_\theta =$ 29.19 kg m⁻³ and O₂ ~ 198 mmol m⁻³) reflect the contribution of dense water of Aegean origin, the CDW, now situated at about 1500
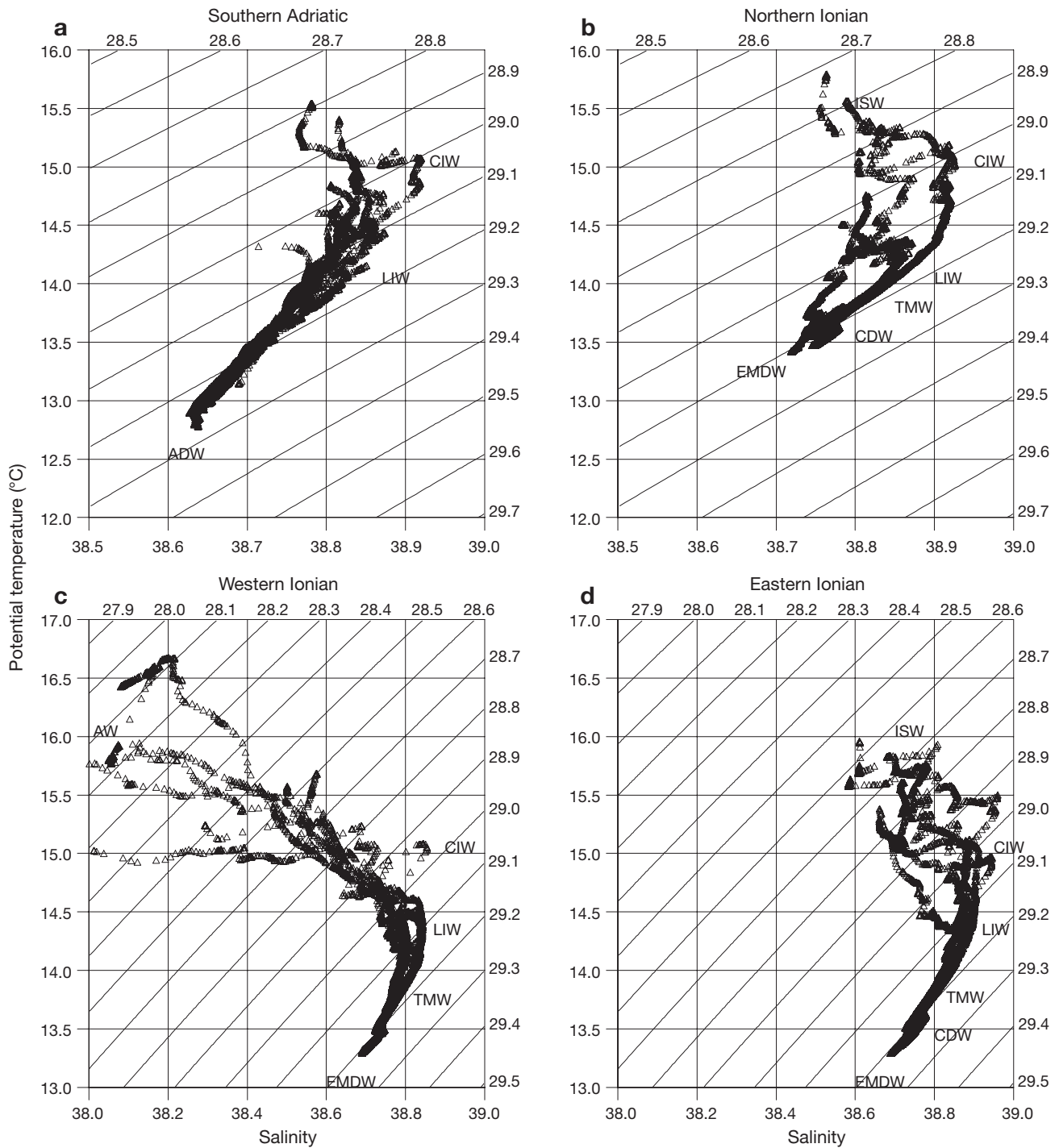
Fig. 8. θ-S diagrams constructed with CTD data from stations in the (a) southern Adriatic, (b) northern Ionian, (c) western Ionian, and (d) eastern Ionian (cf. Fig. 1b) during SINAPSI-4. See Table 1 for acronyms of water masses discussed in text

to 2000 m (Figs. 8d & 9a). These modifications are lower than those observed at the same position near the bottom layer during the mature phase of the transient (Klein et al. 1999).

The hydrochemical characteristics of the different SWTs have been derived from the property-property plots constructed with the complete set of parameters (Fig. 9). The near-surface AW and ISW are characterised by oxygen maxima related to the biogeochemically defined minima of nutrients. The AW is described by 2 SWTs, denominated AW1 and AW2, which consider the distinctive characteristics in the photic and
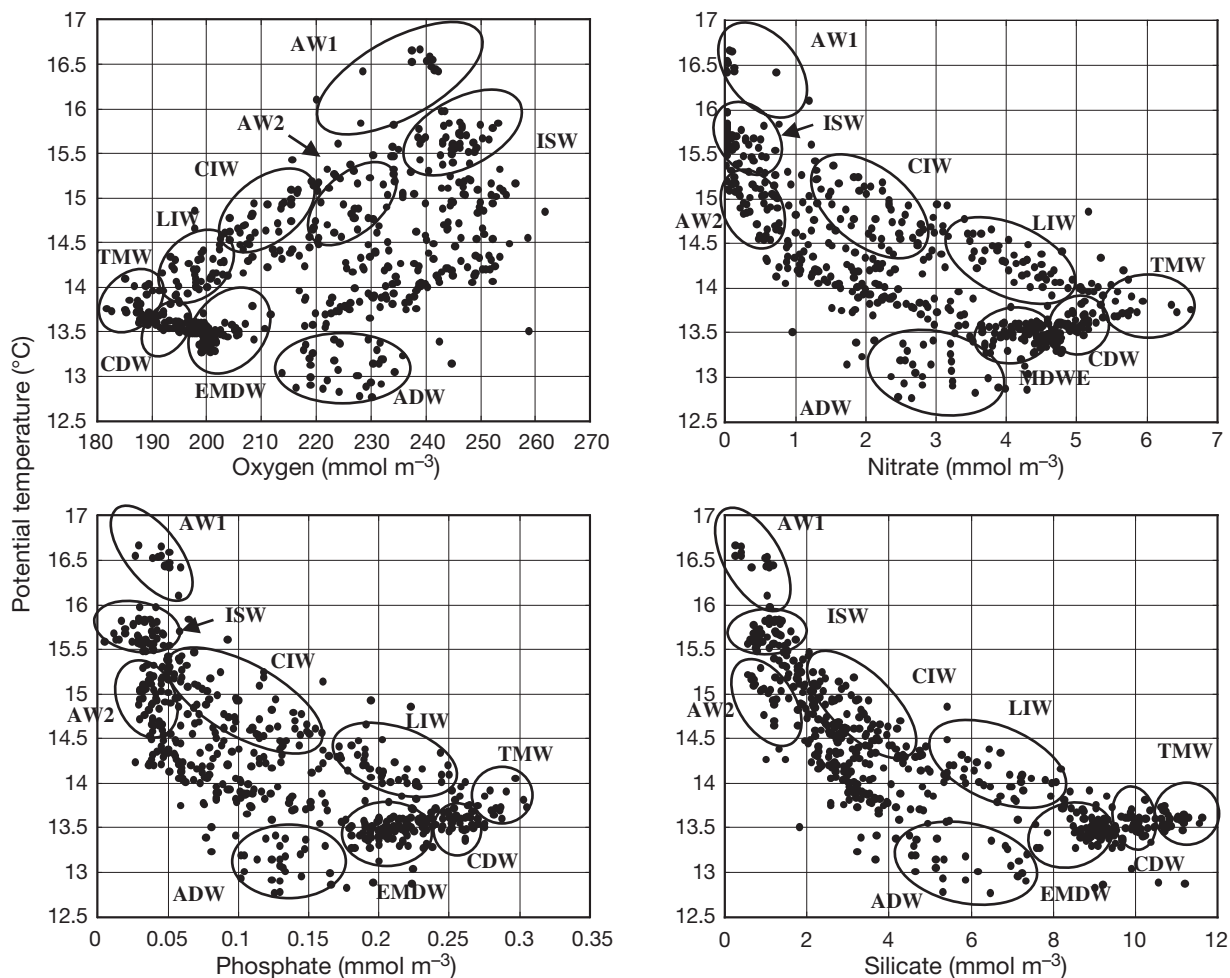
Fig. 9. Property-property plots constructed with hydrographic data from all bottle casts for (a) oxygen, (b) nitrate, (c) phosphate and (d) silicate versus potential temperature. Ellipses enclose properties of different water masses (see Table 1 for acronyms)

aphotic layers. In the temperature range 14 to 15.5°C, the CIW appears richer in oxygen and poorer in nutrients than the LIW (Fig. 9). In the deep layer, cold waters (13.5 to 14°C) associated with the minima of oxygen and the maxima of nutrients indicate the TMW. Below the TMW, the deep and bottom waters (i.e. the ADW, EMDW and CDW) show an inversion towards higher values of oxygen and lower values of nutrients.

Table 1 lists the characteristics of SWTs and the parameter weights used in the OMP analyses. The final values are derived from extrapolation as idealized end-members of the mixing lines. The vertical distribution of the mass fractions (%) relative to the different water types are depicted along specific sections (Figs. 10, 11 & 12) that correspond to the sections illustrated in Figs. 2, 4 & 5. In the figures, only fraction values greater than 10% are shown, and dots indicate the position of the hydrographic stations and related water samples. These quantities may be affected by a

possible source of errors derived from the characterization of source water types, from the analytical imprecision of water sample analysis and from the deviation of the mixing curve assumed as linear transition between idealized end-members of the mixed lines. In practice, the definition of water types and the correct weighting of parameters relative to each other were adjusted to minimise the mass conservation residuals of the fit (Mackas et al. 1987), which in our case resulted within 8%.

The water mass fractions along the section at the nominal latitude of 36° N (Fig. 10) compare well with the distribution of salinity and oxygen as shown in Fig. 2. The 8 water types considered in this section are: AW_1, AW_2, ISW, CIW, LIW, TMW, EMDW and CDW. The AW is shown as the sum of the contributions from water types AW_1 and AW_2 and manifests the highest fraction at the west, while the ISW highest fraction is found at the east (Fig. 10a,b). Further down, the CIW (Fig. 8d) appears as patches that interweave with

Table 1. Properties and parameter weights for the source water types used in OMP analysis. AW: Atlantic Water; ISW: Ionian Surface Water; CIW: Cretan Intermediate Water; LIW: Levatine Intermediate Water; TMW: Transitional Mediterranean Water; ADW: Adriatic Deep Water; EMDW: Eastern Mediterranean Deep Water; CDW: Cretan Deep Water

| Parameter/Water Types	AW_1	AW_2	ISW	CIW	LIW	TMW	ADW	EMDW	CDW	Weights
Pot Temperature (°C)	17.0	15.0	16.0	15.5	14.5	13.75	12.92	13.3	13.6	25
Salinity	37.6	38.6	38.8	39.0	38.9	38.75	38.65	38.69	38.78	25
Oxygen (mmol m^{-3})	250	220	260	215	200	180	232	200	198	20
Phosphate (mmol m^{-3})	0.02	0.06	0.02	0.06	0.20	0.30	0.12	0.20	0.25	2
Nitrate (mmol m^{-3})	0.05	0.50	0.05	1.50	4.00	6.50	2.80	4.00	5.00	2
Silicate (mmol m^{-3})	0.2	1.0	1.0	2.0	5.0	12.0	6.0	8.0	9.5	2
Pot.Vorticity (10^{-8} m^{-1} s^{-1})	0.03	0.04	0.01	0.15	0.01	0.02	0.02	0.	0.	1
Mass conservation	1	1	1	1	1	1	1	1	1	25
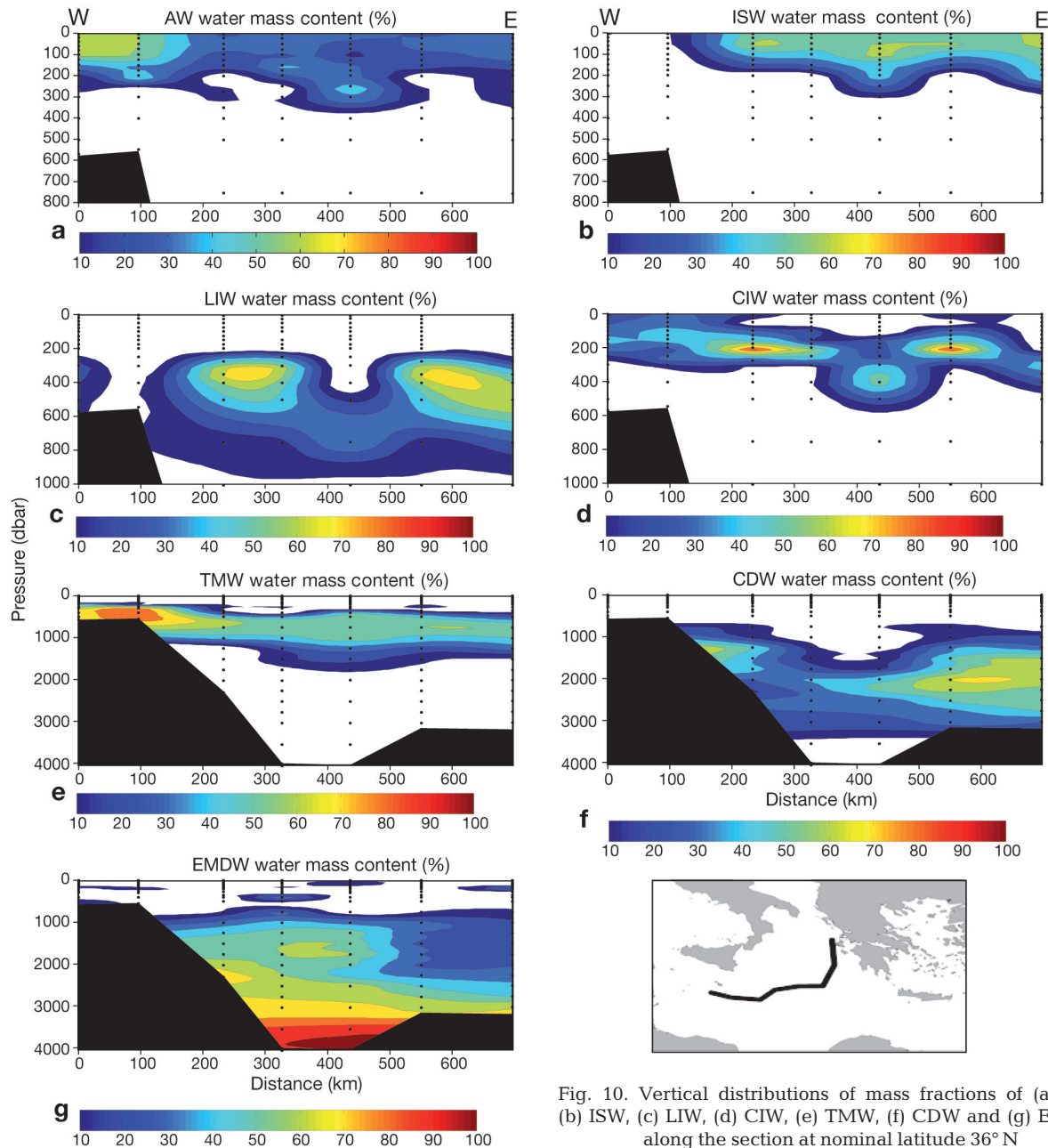
Fig. 10. Vertical distributions of mass fractions of (a) AW, (b) ISW, (c) LIW, (d) CIW, (e) TMW, (f) CDW and (g) EMDW along the section at nominal latitude 36° N

LIW (Fig. 10c). Considerable amounts of the CIW are brought to shallower depth, while the LIW breaks down into smaller quantities that recirculate at intermediate levels because of strong sub-basin scale dynamics. The contribution of the TMW (Fig. 10e) compares well with the oxygen minima in Fig. 2; in addition, a large fraction of TMW intrudes over the Sicily Strait and seems to flow further into the Western Mediterranean, where variations in the deep water characteristics in the Tyrrhenian Sea have been related to the EMT (Astraldi et al. 2002).

Below this layer, a considerable portion of EMDW appears at latitude 36° N from 2000 m to the bottom (Fig. 10g). The Ionian abyssal layer contains EMDW exclusively, which is of course as it should be since we have defined this SWT using data in this layer. However, the EMDW has a large extension (more than 50% by volume) to the west. In contrast, the CDW dominates on the eastern flank of the section (Fig. 10f) but by a smaller amount. The CDW re-circulates cyclonically in the basin and still appears against the western continental slope at depths shallower than the EMDW. This reflects the fact that the Aegean outflow had weakened around 1995–1997 (Manca & Scarazzato 2001, Theocharis et al. 2002), and it occurs over a density range centred at 29.19 kg m^{-3}, lower than that of the EMDW, causing isopycnal mixing between them for most of the depth range.

The interaction between the Adriatic and Ionian Seas is shown more clearly in Figs. 11 & 12, which illustrate the water mass fractions along the 2 meridional sections that link the Adriatic to the Ionian Sea. The 8 water types considered in this section are: AW2, ISW, CIW, LIW, TMW, ADW, EMDW and CDW. Here we have considered the AW2 exclusively, which flows from south to north in the sub-surface layer and in quantities greater than the ISW (Figs. 11a & 12a). The ISW penetrates more into the northern Ionian at the surface, from where it seems to intrude the Adriatic Sea (Figs. 11b & 12b). A considerable amount of LIW/ CIW occurs both along the eastern and the western section. The CIW (Figs. 11d & 12d) spreads at a depth shallower than that of the LIW; the latter has a thickness of about 300 m centred at 500 m (Figs. 11c & 12c). These water masses meander and exhibit a more continuous pattern along the eastern section (Fig. 12c,d), according to the general cyclonic character of the circulation. The TMW appears at the eastern section with a fraction higher than that at the west (Figs. 11f & 12f). There, the large intrusion of the CDW had greatly contributed to the uplifting of the oldest EMDW of Adriatic origin in the transitional layer (Klein et al. 1999).

The bottom layer appears largely influenced by the ventilation process because of the contribution of dense waters either from the Adriatic and/or Aegean Seas. The ADW reaches the Otranto Strait with a fraction greater than 90% (Fig. 11e); there, a frontal zone is generated with the TMW that flows at the same level over the sill (Fig. 12 f) but in a smaller fraction. The southward penetration of the ADW into the Ionian occurs mostly against the western continental margin, where it mixes with the ambient deep water and transforms into the EMDW (Fig. 11g). In contrast, the CDW flows mostly along the eastern section and fills large volume of water at the northern continental margin (Fig. 12h), even if mixtures of EMDW and CDW appear elsewhere at lower densities.

4.2. Impact on the Adriatic Sea as this region once again became the primary source of deep water

The Ionian and Adriatic Seas have been surveyed twice, in January 1999 and in March-April 2002. A quantitative comparison of salinity and dissolved oxygen fields between the 2 observation periods is shown in Fig. 13. In the southern Adriatic, the salinity increase in the surface and intermediate layers is related to long-term salinity changes in the Ionian Sea (Klein et al. 2000, Manca et al. 2003). Moreover, the increase in both salinity and oxygen in the deep layer (Fig. 13a,b) indicates a combination of different processes, such as intrusion of highly saline water, strong buoyancy fluxes and convection activities in the southern cyclonic gyre. In 2002, the water column over the western continental slope appears also characterised by a moderate increase in salinity and a much stronger dissolved oxygen increase if compared with the situation at the same depth levels during the 1999 survey (Fig. 13a,b). These features, also observed in the past (Bignami et al. 1990, Manca et al. 2002), were attributed to the arrival of much denser waters from the northern shelf region that sink into the deep layer of the southern Adriatic Sea. In fact, the hydrographic and optical properties discussed above (Fig. 3) clearly indicate that the deep-water mass that resides in the southern Adriatic depression has been renewed.

In the Ionian Sea, below the permanent thermocline, the salinity and oxygen increase (Fig. 13c,d) indicates that the LIW has resumed the traditional westward path, while more saline and oxygen-rich CIW mixes with the LIW. In the deep layer, property-property plots (Figs. 8 & 9) have revealed the presence of the biochemically defined TMW and a steady decrease in temperature and salinity toward the bottom. In 2002, the transitional layer appeared less ventilated and shifted to shallower depths, showing a westward extension into the Sicily Strait (Fig. 13d). However, the moderate salinity decrease and oxygen increase from 1000 to
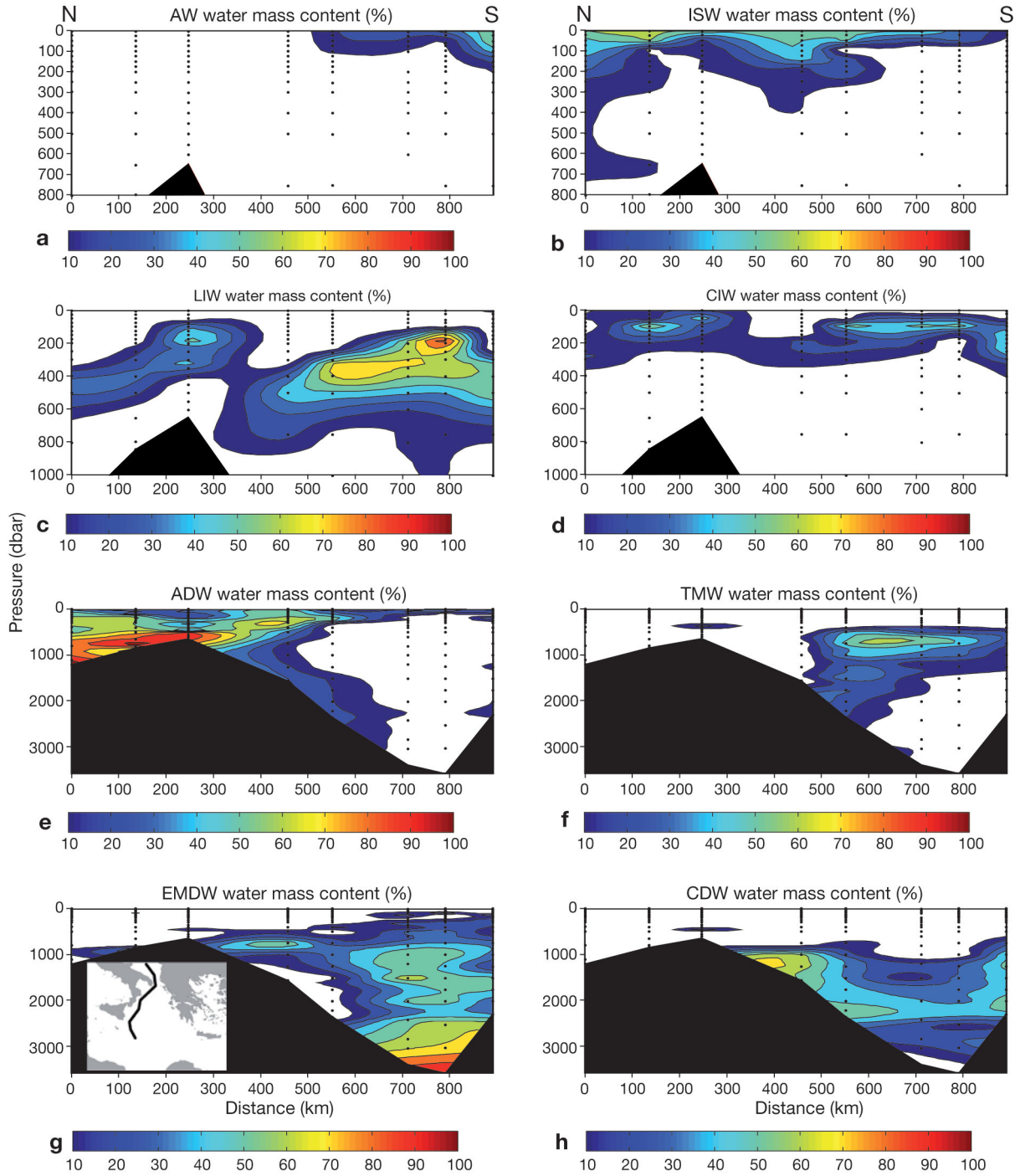
Fig. 11. Vertical distributions of mass fractions of (a) AW, (b) ISW, (c) LIW, (d) CIW, (e) ADW, (f) TMW, (g) EMDW, and (f) CDW along the north-south section at nominal longitude 16–17°E

3000 m in the western and eastern Ionian (Fig. 13c,d) nearly coincide with the ADW and CDW propagations, transported there by a southward and northward current, respectively. The EMDW that resides in the Ionian abyssal layer had the same salinity values as in 1999 but the oxygen was higher in 2002. This indicates north-south movement of the ADW, which strongly contributed to the deep ventilation. The advection of the modified CDW over the Mid Mediterranean Ridge (Fig. 1a) can be ruled out as the cause of the deep ventilation, since the oxygen increase was not accompanied by a parallel salinity increase.
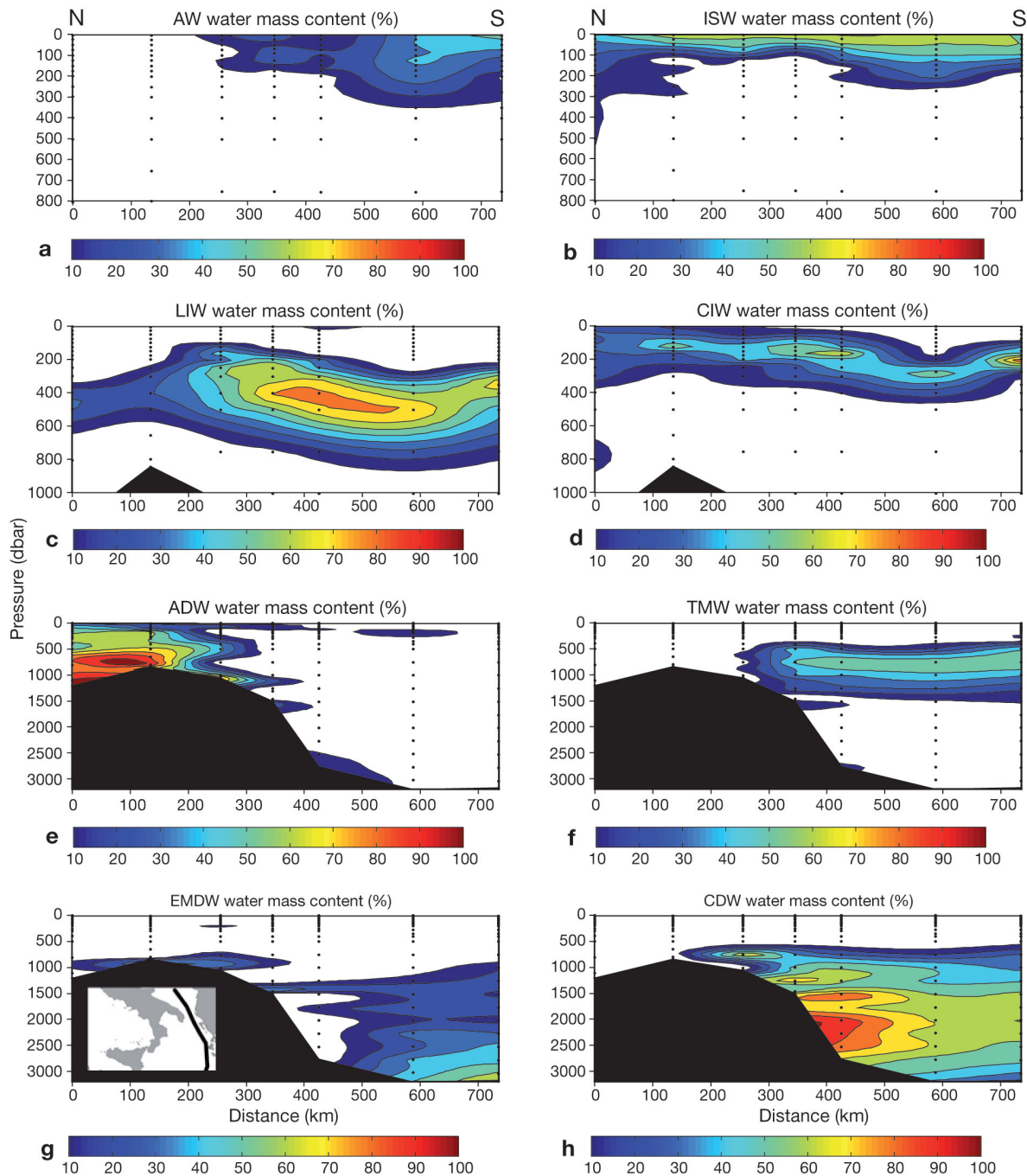
Fig. 12. Vertical distributions of mass fractions of (a) AW, (b) ISW, (c) LIW, (d) CIW, (e) ADW, (f) TMW, (g) EMDW, and (f) CDW along the north-south section at nominal longitude 19–20° E

5. SUMMARY AND CONCLUSIONS

Hydrographic observations conducted in the Adri-atic and Ionian basins in March–April 2002 illustrate the continuity of changes in the thermohaline proper-ties as a consequence of the great Aegean anomaly. These variations deal with the upper, intermediate and deep layers and are only indirectly related to the dense

Aegean outflow. At the time of these observations, the AW is diverted towards the Levantine basin, while the LIW path, which was altered by strong dynamics in the Levantine basin during the early stage of the transient, disperses through the Cretan Passage and enters the Ionian Sea in its southeastern corner, mixing with the CIW. The CIW accounts for a secondary source of saline water characterised by higher oxygen as
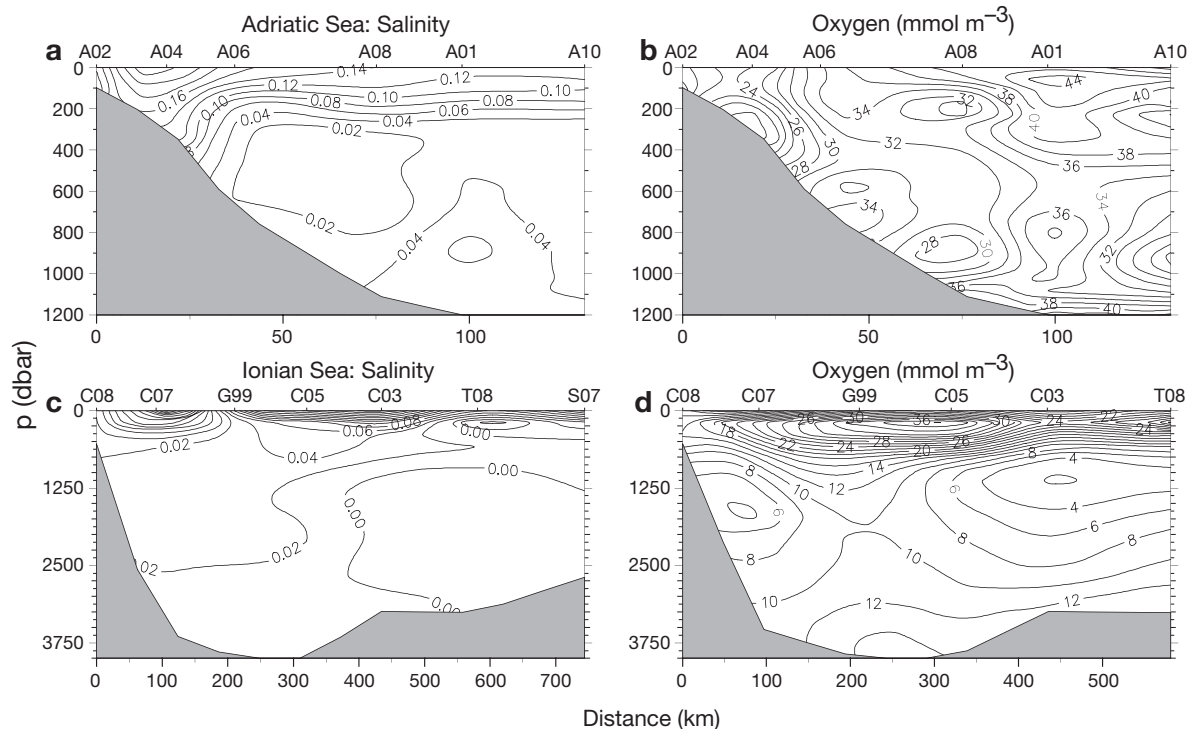
Fig. 13. Differences in salinity (left panels) and oxygen (mmol m^{-3}) (right panels) between 1999 and 2002 in the southern Adriatic Sea (top panels) and Ionian Sea (bottom panels). Positions of CTD stations indicated at the top of the x-axis

well. Its core is warmer (θ ~14.5 to 15.5°C) and saltier (S ~38.9 to 39) than the LIW entering the Ionian Sea, and flows prevalently along the eastern side into the Adriatic Sea.

Oxygen vertical distribution along hydrographic sections has shown the TMW to be a low oxygen and high nutrient carrying water mass, which occupies the transitional layer (800 to 1500 m). In the deep layer, during the main manifestation of the EMT, the CDW overflowed the Cretan Arc Straits. This water mass mixed with the resident bottom water and strongly contributed to salinity and oxygen increase in the bottom layer of the Ionian Sea. Our data show the CDW signature that flows prevalently toward the northern Ionian where it settles at the base of the continental margin. In contrast, the ADW prevalently influences the bottom layer along the western side.

Local thermohaline properties and biochemical characteristics of 8 SWTs appear to be good tracers for calculating the relative mass fractions and mixing coefficients. Multiparameter analysis using hydrographic data clarified the mixing processes that modify the water masses in the deep and bottom layers, and showed how the Adriatic Sea once again became the primary source of deep water in the eastern Mediterranean. Up to 50% of the global volume is comprised of colder, fresher and oxygen-rich dense water that again occupies the Ionian abyssal layer.

LITERATURE CITED

Artegiani A, Bregant D, Paschini E, Pinardi N, Raicich F, Russo A (1997) The Adriatic Sea general circulation. Part II: baroclinic circulation structure. J Phys Oceanogr 27: 1515–1532

Astraldi M, Gasparini GP, Vetrano A, Vignudelli S (2002) Hydrographic characteristics and interannual variability of water masses in the central Mediterranean: a sensitivity test for long-term changes in the Mediterranean Sea. Deep-Sea Res I 49:661–680

Bethoux JP (1989) Oxygen consumption, new production, vertical advection and environmental evolution in the Mediterranean Sea. Deep-Sea Res A 36:769–781

Bethoux JP, Morin P, Madec C, Gentili B (1992) Phosphorus and nitrogen behaviour in the Mediterranean Sea. Deep-Sea Res 39:1641–1654

Bignami F, Salusti E, Schiarini S (1990) Observations on a bottom vein of dense water in the southern Adriatic and Ionian Seas. J Geophys Res 95:7249–7259

Carpenter JH (1965) The accuracy of the Winkler method for dissolved oxygen analysis. Limnol Oceanogr 10:135–140

Carter EF, Robinson AR (1987) Analysis model for estimation of ocean fields. J Atmos. Ocean Technol 4:49–74

Grasshoff K, Erhardt M, Kremling K (1983) Methods of seawater analysis. Verlag Chemie, Weinheim

Hopkins TS (1978) Physical processes in the Mediterranean basins. In: Kjerfve B (ed) Estuarine transport processes. Univeristy of South Carolina Press, Columbia, SC, p 269–310

Josey SA (2003) Changes in the heat and freshwater forcing of the eastern Mediterranean and their influence on deep water formation. J Geophys Res 108:3237, doi:10.1029/2003JC001778

Klein B, Roether W, Manca BB, Bregant D, Beitzel V, Kovacevich V, Luchetta A (1999) The large deep water transient in the eastern Mediterranean. Deep-Sea Res I 46: 371–414

Klein B, Roether W, Civitarese G, Gacic M, Manca BB, Ribera d'Alcala' M (2000) Is the Adriatic returning to dominate the production of Eastern Mediterranean Deep Water? Geophys Res Lett 27:3377–3380

Klein B, Roether W, Kress N, Manca BB and 5 others (2003) Accelerated oxygen consumption in eastern Mediterranean deep waters following the recent changes in thermohaline circulation. J Geophys Res 108:8109, doi:10.1029/2002JC001454

Kress N, Herut B (2001) Spatial and seasonal evolution of dissolved oxygen and nutrients in the southern Levantine basin (eastern Mediterranean Sea). Chemical characterization of the water masses and inferences on the N:P ratios. Deep-Sea Res I 48:2347–2372

Kress N, Manca BB, Klein B, De Ponte D (2003) Continuing influence of the changed thermohaline circulation in the eastern Mediterranean on the distribution of dissolved oxygen and nutrients: physical and chemical characterization of the water masses. J Geophys Res 108:8109, doi:10.1029/2002JC001397

Lascaratos A, Roether W, Nittis K, Klein B (1999) Recent changes in deep water formation and spreading in the eastern Mediterranean Sea. Prog Oceanogr 44:5–36

Leffanue H, Tomczak M (2004) Using OMP analysis to observe temporal variability in water mass distribution. J Mar Syst 48:3–14

Mackas DL, Denman KL, Bennet AF (1987) Least square multiple tracer analysis of water mass composition. J Geophys Res 92:2907–2918

Malanotte-Rizzoli P, Manca BB, Ribera d'Alcalà M, Theocharis A, Brenner S, Budillon G, Ozsoy E (1999) The eastern Mediterranean in the 80s and in the 90s: the big transition in the intermediate and deep circulations. Dyn Atmos Oceans 29:365–395

Manca BB, Scarazzato P (2001) The two regimes of the intermediate/deep circulation in the Ionian-Adriatic Seas. Arch Oceanogr Limnol 22:15–26

Manca BB, Kovacevic V, Gacic M, Viezzoli D (2002) Dense water formation in the southern Adriatic sea and spreading into the Ionian sea in the period 1997–1999. J Mar Syst 33–34:133–154

Manca BB, Budillon G, Scarazzato P, Ursella L (2003) Evolution of dynamics in the eastern Mediterranean affecting water mass structures and properties in the Ionian and Adriatic Seas. J Geophys Res 108:8102, doi:10.1029/2002JC001664

Manca B, Burca M, Giorgetti A, Coatanoan C, Garcia MJ, Iona A (2004) Physical and biochemical averaged vertical profiles in the Mediterranean regions: an important tool to trace the climatology of water masses and to validate incoming data from operational oceanography. J Mar Syst 48:83–116

Marini M, Russo A, Paschini E, Grilli F, Campanelli A (2006) Short-term physical and chemical variations in the bottom water of middle Adriatic depressions. Clim Res 31:227–237

Pinardi N, Korres G, Lascaratos A, Roussenov V, Stanev E (1997) Numerical simulation of the interannual variability of the Mediterranean Sea upper ocean circulation. Geophys Res Lett 24:425–428

Ribera D'Alcalà M, Civitarese G, Conversano F, Lavezza R (2003) Nutrient ratios and fluxes hint at overlooked processes in the Mediterranean Sea. J Geophys Res 108:8106, doi:10.1029/2002JC001650

Roether W, Well R (2001) Oxygen consumption in the eastern Mediterranean. Deep-Sea Res I 48:1535–1551

Roether W, Manca BB, Klein B, Bregant D, Georgopoulos D, Beitzel V, Kovacevic V, Luchetta A (1996) Recent changes in eastern Mediterranean deep waters. Science 271: 333–335

Schlitzer R, Roether W, Hausmann M, Junghans HG, Oster H, Johannsen H, Michelato A (1991) Chlorofluoromethane and oxygen in the eastern Mediterranean. Deep-Sea Res I 38:1531–1551

Seritti A, Manca BB, Santinelli C, Murru E, Boldrin A, Nannicini L (2003) Relationships between dissolved organic carbon (DOC) and water mass structures in the Ionian Sea (winter 1999). J Geophys Res 108:8112, doi:10.1029/2002JC001345

Theocharis A, Nittis K, Kontoyiannis H, Papageorgiou E, Balopoulos E (1999) Climatic changes in the Aegean influence the eastern Mediterranean thermohaline circulation (1986–1997). Geophys Res Lett 26:1617–1620

Theocharis A, Klein B, Nittis K, Roether W (2002) Evolution and status of the Eastern Mediterranean Transient (1997–1999). J Mar Syst 33–34:91–116

Tomczak M (1981) A multi-parameter extension of temperature/salinity diagram techniques for the analysis of non-isopycnal mixing. Prog Oceanogr 10:147–171

Tomczak M, Large DGB (1989) Optimum multiparameter analysis of mixing in the thermocline of the eastern Indian ocean. J Geophys Res 94:16141–16149